

EXPERIMENTAL PERMEABILITY OF SINTERED POROUS MEDIA MULTILAYER

Gustavo George Verdieri Nuernberg, verdieri@labtucal.ufsc.br

Juan Pablo Mera Florez, jpablo@labtucal.ufsc.br

Department of Mechanical Engineering (Heat Pipe Laboratory).

Federal University of Santa Catarina -UFSC

Technological Center; POB: 476 – Trindade, Zip code: 88040-900, Florianópolis/SC – Brazil.

Tel: +55 (48) 3721-9937; Fax: +55 (48) 3721-7615

Paiva, K; Almeida, R. S. M; Mantelli, M. B. H.; *Klein, A. N.; Reis, F.; Santos, J.B.

kpaiva@labtucal.ufsc.br; renato@labtucal.ufsc.br; marcia@emc.ufsc.br; klein@emc.ufsc.br;

flavio.emat@gmail.com; jb_engmat@yahoo.com.br.

Department of Mechanical Engineering (Heat Pipe Laboratory); *(Materials Laboratory).

Federal University of Santa Catarina -UFSC

Technological Center; POB: 476 – Trindade, Zip code: 88040-900, Florianópolis/SC – Brazil.

Tel: +55 (48) 3721-9937; Fax: +55 (48) 3721-7615

***Abstract.** Mini heat pipes (MHP) are employed in thermal control of electronic components, such as notebook processors and video display boards. Sintered porous media is used in mini heat pipes to perform the capillary transport of the working fluid from the condenser to the evaporator section. In this matter, there has been a development in porous media, such as the sintered multilayer, to intensify the heat transfer capacity in mini heat pipes. The measurement of permeability is an important parameter for modeling the mini heat pipes behavior. This paper presents an experimental measurement of the permeability of sintered porous multilayer using argon as the working gas. The measurement equipment was developed at LABTUCAL/UFSC. This apparatus measures the gas flux through the sample, while recording the pressure drop. Atomized copper powder was selected to build cylindrical samples of 0.020m in diameter and 0.025m in length. Commercial powder PAC and PAM, produced by METALPÓ Ind., was used for this study. The porous media is composed of two layers with a different particle size range (average size 20 and 50µm to PAC and PAM respectively) and a third central layer as the interface of those layers. The interfacial characteristic length was determined by applying statistical images analyses using the software IMAGO®. Porosity and frequency correlations were employed as parameters of evaluation. A possible relationship between the measured interfacial characteristic length and the particle average size was identified. The experimental results were compared to models presented in literature, relating the influence of each layer to the total effective permeability.*

Keywords: multilayer porous media, mini heat pipes, effective permeability.

1. INTRODUCTION

Mini heat pipes (MHP) basically consist of small heat pipes that are able to efficiently transport relatively high amounts of thermal energy. They can be employed as thermal control devices in the aerospace industry, for cooling of electronic equipment, in the automotive industry, and among other applications (Faghri, 1995). The behavior of MHP with sintered wick structure has been studied by LABTUCAL (Heat pipe laboratory).

For instance, with portable computers the increase of their data processing capacity together with the decrease of their size and weight lead to the development of small processors and other electronic components that dissipate high amounts of concentrated heat. Actually, the heat dissipation of electronic components is a major limitation for the development of faster and smaller computers. Computational development has increased the data processing and reduced the components size. MHP are, basically, an evacuated metal case with a capillary structure in it to transport the working fluid. Like a classic heat pipe, the mini heat pipe can be divided into three sections: the evaporator section, an adiabatic section, and a condenser section. MHP with a sintered wick structure have been studied in the Heat Pipe Laboratory since 2005.

The main objective of the present work is to study and measure the effective permeability in multilayer porous media. Porous media permeability is an important factor to consider in the MHP project, particularly to preview the fluid pressure drop in the condenser section and the pressure distribution in the whole MHP. According to Faghri (1995) permeability can be defined as a parameter that describes the relationship between pressure drop and the mass transfer through a porous media. It is usual to use semi-empirical correlations based on experimental data to presume the system permeability. These correlations depend on the particle size, diameter, and porosity of the sintered porous media. However, employing correlations to model the permeability of MHP proves not so accurate (Faghri, 1995). Experimental measurements are indicated for precision. Homogeneous porous media that show a low effective permeability generally indicates that this material has a tiny porous ratio, and usually a low porosity. This aspect indicates a high capillary pressure, which increases the capillary pumping and the thermal resistance of the whole

system. Homogeneous porous media with high porosity has a high effective permeability with low capillary pressure and low thermal resistance. A multilayer porous media wick is a porous media material with two distinct pore size distributions; small pores that are capable of providing a high level of capillary pumping and larger pores capable of providing a large free path for vapor.

The literature specifies a great number of mathematic models to determine the effective permeability, the most important model is Darcy's law. A variant of Darcy's law is Forchheimer's model, this model is more accurate, considering the flow regime.

In this work, the low velocity of the gas flow indicates that Darcy's law is better applicable in each porous media layer under consideration. Darcy's law is valid for slow flow through low permeability media. This model was used because it ignores inertial effects, which arise due to the microstructure of the medium and curvilinearity of the flow path, and ignores the viscous shear effects, which inevitably arise when a viscous fluid flows near a macroscopic solid boundary on which a no-slip condition must be imposed (Ford and Handam, 1998).

This paper presents an experimental measurement of the permeability of sintered porous multilayer using argon as the working gas. The measurement equipment was developed at LABTUCAL. This apparatus measures the gas flux through the sample, while recording the pressure drop. Atomized copper powder was selected to build cylindrical samples of 0.020 m diameter and 0.025 m length.

For this study, commercial copper powder named PAC and PAM has been used. The porous media is composed of two layers with different particle size ranges (average size 20 and 50µm to PAC and PAM respectively), and a third central layer as the interface of those layers. The interfacial characteristic length was determined by applying statistical image analyses using the software IMAGO[®]. Porous media porosity and frequency correlations of the digital image were employed as parameters.

2. THEORY FUNDAMENTS

2.1. Permeability

Permeability is the term used for the conductivity flow of a Newtonian fluid through a porous medium. (Dullien, 1979). The permeability unit is called "Darcy". A Darcy in a porous material could be defined as a pressure difference of $1,013 \times 10^5$ Pa will produce a flow rate of $1 \text{ cm}^3/\text{s}$ of a fluid with $1 \text{ mPa}\cdot\text{s}$ viscosity through a cube having sides 1 cm in length. Thus the Darcy law could write, according to the Equation (1):

$$\frac{dp}{dx} = -\frac{\mu v}{K} \quad (1)$$

Where K is a constant of proportionality called permeability, dp/dx represents the pressure gradient in the flow direction, μ is dynamic viscosity of fluid and v is superficial flow velocity (Kececioclu and Jiang, 1994).

Permeability could be described as the relationship between pressure drop and the mass transfer through the porous media (Faghri, 1995). It can be observed that Darcy equation disregards density effects on the fluid pressure drop. As a consequence, the fitted curve is only useful within the fitting range and the curve extrapolation might not be valid for other fluids or other flow situations.

According to Innocentini *et al.* (1999), Forchheimer equation Eq. (2) was used to calculate the permeability in ceramic foams applying air flow as the working fluid. Use of the Forchheimer equation in such a way considers the nonlinearity of the pressure gradient with the fluid velocity, this calculation is done by a simplified form of the Forchheimer equation:

$$\frac{P_i^2 - P_0^2}{2PL} = \frac{\mu}{k_1} v_s + \frac{\rho}{k_2} v_s^2 \quad (2)$$

Where, P_i is the absolute pressure at the gas entrance and P_0 the absolute pressure at the gas exit of a sample with thickness L . P is the pressure at which fluid velocity (v_s), fluid density (ρ), and the fluid viscosity (μ). The constants k_1 and k_2 are named respectively, the Darcian and non-Darcian permeabilities. The term $\mu v_s / k_1$ of Eq.(2) represents the contribution to flow resistance due to the friction between fluid layers and the pore walls. The term $\rho v_s^2 / k_2$ represents the contribution of inertia and turbulence (Innocentini, 1999).

The parameters k_1 and k_2 represent the constants polynomial of interpolation, from experimental curve $v_s \times (P_i^2 - P_0^2)/2PL$. The permeability k_1 and k_2 may change depending on the range of experimental points used to derive the Forchheimer equation curve. The results obtained by this approach have a greater variation for the constant k_1 to k_2 .

The permeability effect related to the Darcy number in multilayer porous media as done by Allan *et al.* (2009). They made the solution of the velocity profile for a porous medium composed of two layers of different porosities, and a third layer, considered as an interface and other case like a free channel. In a first configuration, the layers are modeled based

on the Forchheimer equation Eq. (2), and the central layer is modeled based on the Brinkman Equation (4). In a second configuration in which the region outside of the two porous media are modeled similarly to the first setup, but with the central channel the flow is considered fully developed and governed by the Navier-Stokes equation. These equations were expressed as a function of Reynolds number and Darcy. Velocity profiles of both configurations were analyzed, fixing the number of Darcy and ranging Reynolds. Likewise the results were compared fixing Reynolds number and changing the Darcy number for each configuration. As the number of Darcy in the outer layers varies the speed does not change the central region. The Reynolds number's change generates an increase in the velocity of flow in the central region.

Other authors have studied the flow through the layers by numerical solution of transport equations, using as a model Darcy-Forchheimer-Brinkman (DFB) Eq. (5) and Darcy-Lapwood-Brinkman (DLB) Equation (4). Ford and Hamdan (1998), numerically solved the flow through a porous medium composed of two layers of different permeability, The upper and lower layer are bounded by solid, impermeable walls on which a no-slip condition is valid. Three different cases were studied, the first case, where the flow through the two layers with different permeability are governed by the DLB model, in the second case the flow through two layers with different permeability is governed by the DFB model, and finally a third case in which flow through a layer is governed by the DLB model by model and another layer DFB.

The main conclusions that characterize flow through composite porous layers are as follows: for low permeability, an increase in the permeability is accompanied with an increase in both the velocity and the shear stress at the interface and when employing the DFB model, the viscous shear term is important only near the macroscopic solid walls (Ford and Hamdan, 1998).

The viscous fluid steady-state flow through a porous domain is governed by the continuity Eq. (3) and momentum Eq. (4) of the form:

$$\nabla \cdot v = 0, \quad (3)$$

$$\rho(v \cdot \nabla)v = -\nabla p + \mu \nabla^2 v - \left\{ \mu v / k + \rho C_d v |v| / \sqrt{k} \right\} \quad (4)$$

Where v is the velocity vector, ρ is the density of the fluid, μ is the viscosity, p is the pressure, k is the permeability, ∇ is the gradient operator and ∇^2 is the Laplacian operator (Ford and Hamdan, 1998).

Equation (4) is recognized as the DFB model, and is compatible with the occurrence of a microscopic boundary. When C_d is set to zero, Equation (3) takes the form:

$$\rho(v \cdot \nabla)v = -\nabla p + \mu \nabla^2 v - \mu v / k \quad (5)$$

The Eq. (5) is known as DLB equation. The mathematical model proposed was based in this equation (Ford and Hamdan, 1998).

2.3 Image analysis

Mathematically, a monochrome digital image is represented by a function $f(x,y)$ of luminous intensity of gray levels of each point (pixel) image. Similarly, colored images have a specific function for each "band" of frequencies, for example, the standard (Red-Green-Blue) RGB. However, most techniques of image processing are applied only to monochrome images. (Marques Filho and Vieira Neto, 1999).

The image processing can be basically separated into four steps: image acquisition, preprocessing, segmentation, pattern recognition, and quantification. (Fernandes, 2002). The image is treated and compared with shapes and patterns previously established for the quantification of the desired characteristics (Marques Filho and Vieira Neto, 1999).

2.1 Binarization by gray histogram

One of the most often used segmentation methods, gray histogram binarization, is based on the gray levels of pixels constituting the image. A threshold level is chosen from which all pixels below this level will be transformed into black and the other white, separating the image into two distinct phases. Figure 1. shows micrographs of a porous structure, in RGB format, and binarized. In the binarized image, particles are represented by the white phase and the black phase represents the pores.

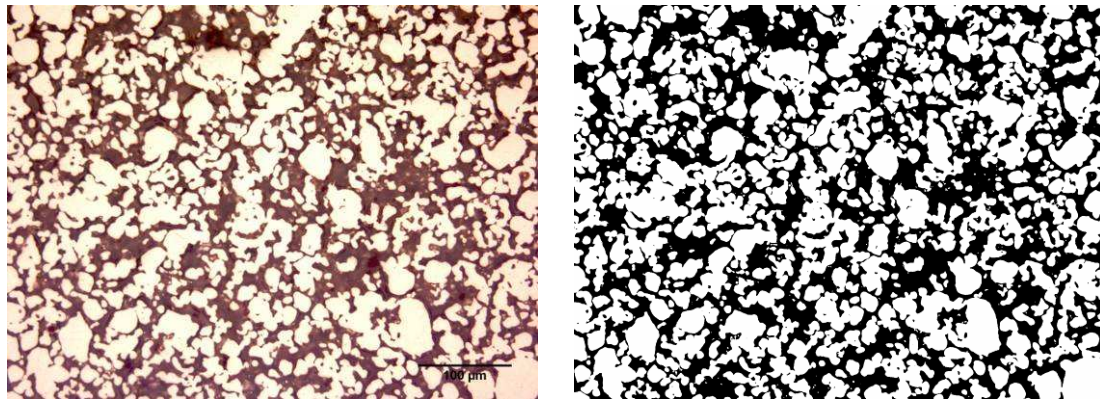


Figure 1. RGB image (left) and binarized image (right).

2.2 Statistical image analysis

In a binary image, there is a statistical function to each two phases, called $Z_{\mathcal{J}}(x)$, equal to 1 if x is part of phase \mathcal{J} , and 0 if not. According the equation, (Fernandes, 2002).

$$\phi_{\mathcal{J}} = |Z_{\mathcal{J}}(x)| \quad (6)$$

Where $\phi_{\mathcal{J}}$ is defined as the first moment of $Z_{\mathcal{J}}(x)$. In a porous media, $\phi_{\mathcal{J}}$ can be interpreted as its porosity, since it represents the probability of a pixel belonging to a pore. The second moment of the function phase \mathcal{J} is defined as the frequency correlation. As show in the Equation (5) bellow, (Fernandes, 2002)

$$C_{\mathcal{J}}(u) = |Z_{\mathcal{J}}(x)Z_{\mathcal{J}}(x+u)| \quad (7)$$

The correlation graphic (Fig. 2) indicates the probability of two distinct pixels, separated by a distance u in an arbitrary direction, to belong to the same phase \mathcal{J} .

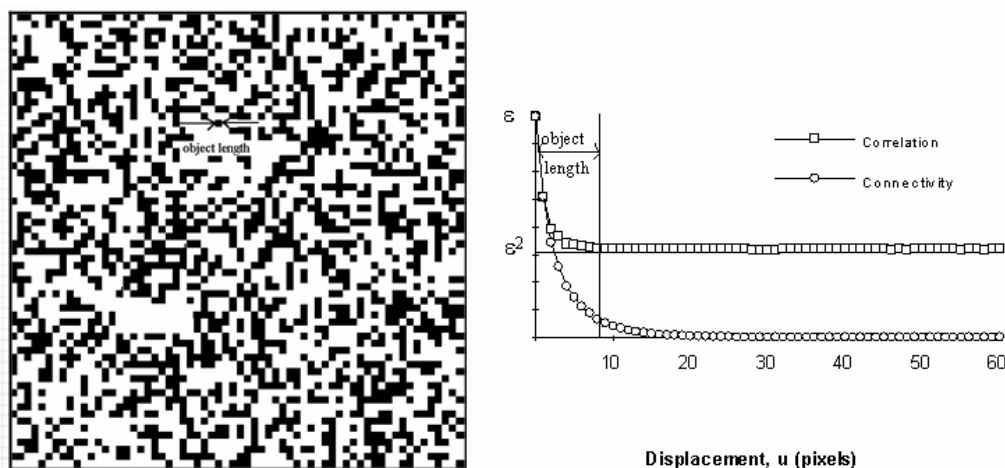


Figure 2. Binarized image frequency correlation (Fernandes, 2002).

4. INVESTIGATED MATERIALS AND EXPERIMENTAL PROCEDURE

Atomized copper powder was employed during this study, according to Fig. 3, as constituent to produce the porous media. This specific material was selected, because it is commonly used to fabricate porous structure in MHP. A characteristic of copper powder is the high thermal conductivity, allied to the low cost, of this powder and no chemical reaction when this material is in contact with the typical mini heat pipe's working fluid. These powders have

commercial names (PAC and PAM), this paper will use the same nomenclature. PAC has a fine particle size and PAM has a coarse particle size.

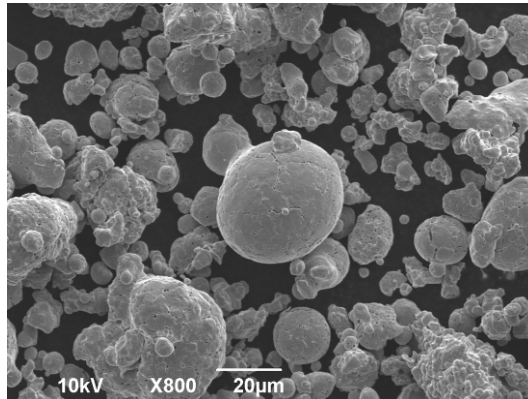


Figure 3. Electronic microscopy image of powder PAC x800

Each sample was made using a loose sintering process. The sample was deposited inside a cast Fig. 4 made by stainless steel 304, cooper has no chemical interaction to stainless steel and this is an important characteristic to build the samples. The sintering process was conducted in a vacuum furnace with a controlled atmosphere of commercial H_2 at the Materials Laboratory, with a working pressure of 0.1 Pa approximately. The heating rate was 4.6 K/s until the temperature of 1123K, where the samples stayed for more 3000 s. That heating curve was the same as applied to produce MHP at the LABTUCAL to make the braze diffusion to seal the heat pipes. As a consequence of the sintering process, the samples underwent a mild contraction, facilitating its removal from the array of stainless steel. The final dimensions of the specimens were measured with a caliper, (Mytutoyo brand), with a resolution of 0.01 mm.

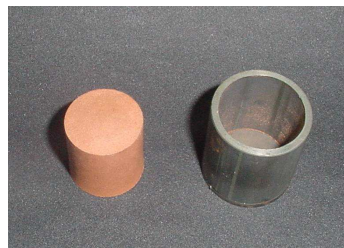


Figure 4. Porous media and matrix

4.1 Permeability measurement

Each sample was covered with an epoxy resin and positioned inside the apparatus sample holder. An apparatus image can be seen in Fig. 5. Argon was used as the working gas and its properties are obtained from EES software. Although the temperature inside the apparatus was not verified, the room temperature was measured to identify the properties of the fluid. As the gas flowed through the sample, a differential transducer was employed, (Omega, model PX409-015DWUV), to measure its pressure drop. The measurement of the gas velocity was made using a standard glass tube, with millimeter graduation. As the gas travels through the sample, it's transported to the standard glass tube, according with Fig. 6, and its flow was determined by measuring the bubble dislocation during a specific time using a chronometer. An acquisition system, (Agilent, model 34970A), was used to determine the differential pressure value. Furthermore, every sample's porosity was measured according to the Archimedes' principle method.

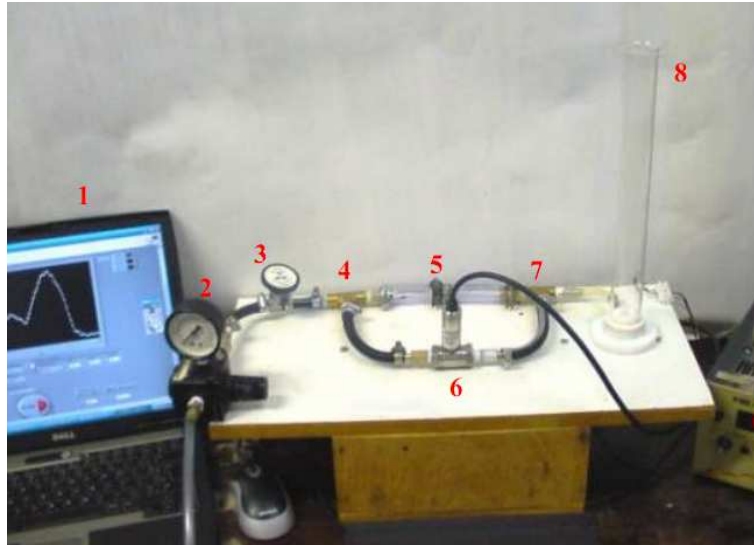


Figure 5. Apparatus; (1) computer to data acquisition, (2) gas inlet control valve, (3) ratio control valve, (4) pressure measurement before sample, (5) sample holder, (6) differential transducer, (7) pressure measurement after sample, (8) glass tube.

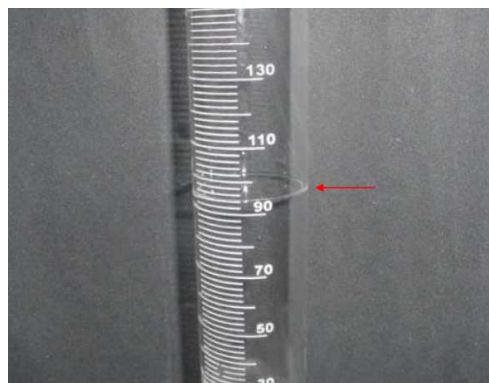


Figure 6. Bubble difference, during the gas flow.

4.2 Image processing

The porous media samples were submitted for a metallographic process, to get a flat surface, free of scratches so that the acquisition of appropriate images by optical microscopy (OM) was possible. This process was used, to obtain a better digital image quality, scratches produce inaccuracies during the measure of the properties in porous media, employing the image analysis. The software could read the scratches like a kind of pore, increasing the level of porosity inside the porous media. The specimens were sectioned in the transversal direction and embedded in acrylic resin by vacuum impregnation; the vacuum impregnation was realized to preserve the porous structure, without the impregnation process the porous structure could be deformed, during the polishing step. The specimens were polished with sandpaper with grain size from 150 to 2000 mesh, and after that step, the samples were polished with alumina with 0.3 μm grain size, followed by diamond paste with 0.25 μm grain size, taking care to not close or open the pores.

The digital image acquisition was performed with a reflected light microscope at the Characterization Materials Laboratory (LCM). Digital images were taken from 20 different regions of each sample, using objective lenses at magnifications of 5, 10, 20, 50, and 100 times.

It is difficult to measure the thicknesses of the two layers as there is an undefined transition region between the layers. To overcome this problem, three distinct regions were considered. The first layer corresponds to an infinitely thick homogeneous porous layer (PAM), a central region, corresponding to the interface between layers, with finite thickness, and a second infinitely thick homogeneous layer (PAM). To measure this transition region, the image was segmented into several "slices" with a thickness of 100 μm . Then a frequency distribution of each slice was made. This analysis of frequency distribution consists in the calculation of the probability of finding a black pixel (porous) in distance $Ux(\mu\text{m})$. When the frequency distribution curves for each slice chance of pattern, one can consider that the

material structure is changed. The process started from the region with higher porosity until three distinct regions could be observed. Figure 7 shows an optical microscopy image of the layered porous media and its interface region.

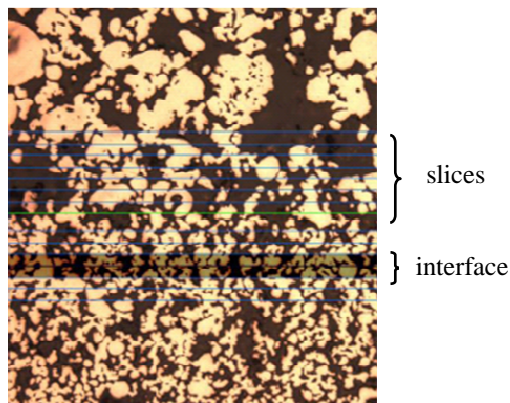


Figure 7. Layers porous media, measure of thickness interfacial layer.

The image analyses was employed to determinate the porosity of each layer and to identify and describe the interface between them. The software Imago[®] was used, this software was developed in association at UFSC and ESSS Software Company.

5. RESULTS

Table 1. shown below indicates the results obtained during the first step of characterization, evaluating each type of porous structure apart. The powder is characterized by the amount of particle which presents diameter up to a certain value. For instance, particle size 50% equal to 20.89 to PAC means that 50 % of the PAC particles have diameters up to 20.89 μm . These results were used to calculate the effective permeability utilizing Darcy's law.

Table 1. Materials characterization

Characteristic materials	PAC	PAM
Diameter sample (m)	2.01E-02	2.01E-02
Area (m^2)	3.173E-04	3.173E-04
Particle size 50% (μm)	20.89	49.04
Porosity ϵ	0.41	0.52
Porosity Imago [®]	0.42	0.51
Length (m)	2.2450E-02	2.2450E-02

The highlighted region in Fig. 8 is the interfacial layer, with a thickness of 70 μm and 48% porosity. In this work, it was observed that the interfacial layer thickness is approximately the sum of both types of powder's average particle size.



Figure 8. Multilayer porous media and interface layer.

Figure 9 shows the correlation frequency of each layer. Because it is not a phase of "homogeneous", the correlation of the interfacial layer is twisted.

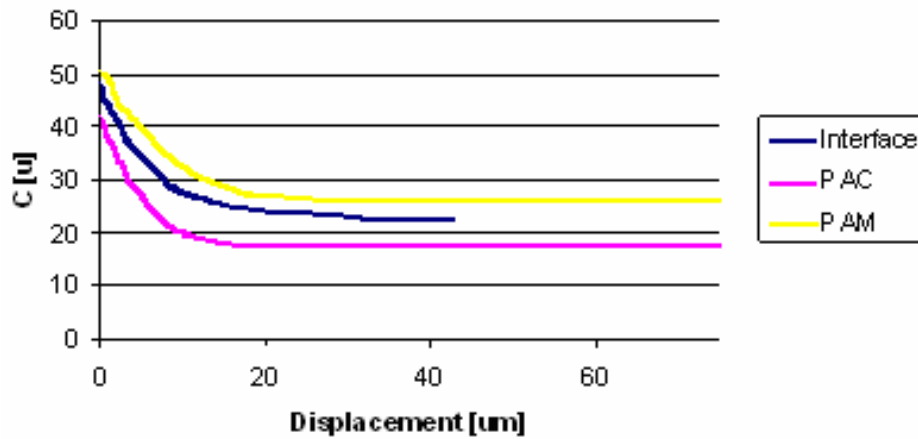


Figure 9. Correlation frequency to each layer porous media.

According to the experimental results Tab. 2, the effective permeability of the two layer sample was approximately the same as the PAM sample, as the fluid tends to flow through the region of higher permeability. As described in a work presented by Ford and Handam (1998), where a numerical solution of the Darcy-Lapwood-Brinkman (DLB) model was proposed, employing the finites differences method, to show the behavior of the velocity profile against the thickness of layers with different permeability relations. Figure 10 shows the graph plotted by fixing the permeability of one layer and increasing the other.

Table 2. Experimental results of permeability

Sample	Permeability (m ²)
PAM	2.89E-12
PAC	3.71E-13
PAM50PAC50	2.45E-12

Additionally, since Reynolds number is relatively low ($Re < 0.5$), Darcy's law is sufficient to describe the slow liquid flow through the sample. So, it is reasonable to ignore inertia effects due microstructure of the medium and the viscous shear effect. Therefore, this experiment was unable to measure the influence of the third interface layer.

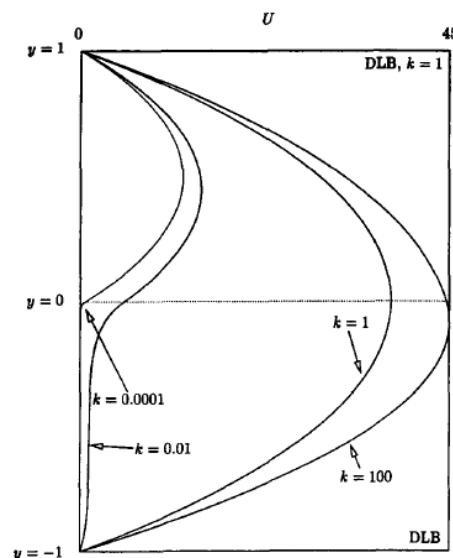


Figure 10. Velocity profile for DLB/DLB composite layers. (Ford and Hamdan, 1998)

According to Catton *et al.* (2010), another way to evaluate the results is to make an analogue between an electrical resistance circuit and a “hydraulic” resistance circuit. Figure 11 represents this circuit, containing three resistances in parallel, both layers (PAC and PAM), and the interface.

Based on the experimental results, it was possible to determinate the equivalent hydraulic resistance. As it is observed in Tab. 3, section PAM presented a resistance way lower compared to PAC and the interface. So, the equivalent hydraulic resistance of the system is governed by PAM, since it is the easiest way for the fluid to flow.

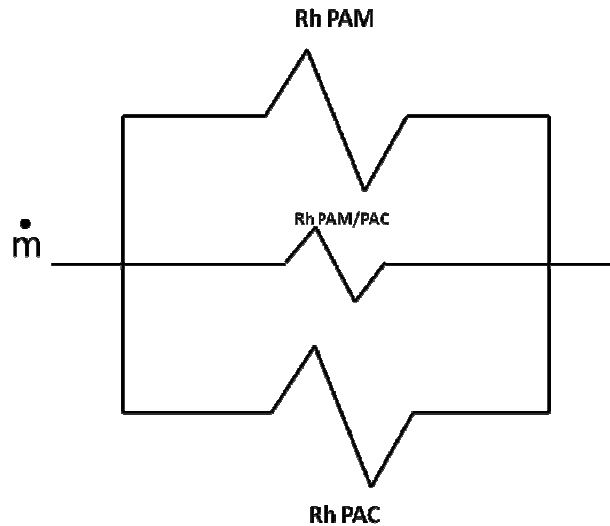


Figure 11. Equivalent hydraulic circuit.

Table 3. Equivalent hydraulic resistances

Rh_PAC	Rh_PAM	Rh_PAM/PAC	Rh_total
5.247E+09	6.36E+08	1.792E+11	5.950E+08

5. CONCLUSIONS

- Based on the frequency correlation theory, it was possible to determinate the interfacial layer thickness, at multilayer porous media;
- Using the image analysis procedure, it was possible to measure the porosity of each layer, and it was possible to measure the interfacial region;
- A study to determinate an analytical solution of fluid flow through a porous media, based on DLB model, was preformed. However, these solutions were not implemented and so they are not presented in this work;
- Experimental data were compared with the numerical solution of DLB and hydraulic resistance, presented by literature;
- The developed apparatus was only able to measure a flow regime in a small range of Reynolds numbers;
- The influence of the interfacial layer on the effective permeability was not able to be detected in this range of velocity.

6. ACKNOWLEDGEMENTS

We would like to acknowledge the National Council for Scientific and Technological Development (CNPq) for financial support through Universal Project and scholarships. Coordination for the Improvement of Higher Level Personnel (CAPES) for the financial support via scholarships. We extend our acknowledgment to EEES Software Company for supplying the image analysis software IMAGO[®] license.

7. REFERENCES

Allan, F.M., Hajji, M.A., and Anwar, M.N., 2009 “The Characteristics of Fluid Flow Through Multilayer Porous Media”, Journal of Applied Mechanics, Vol. 96, January 014501-1/014501-7.

- Catton, I., Amouzegar, L. and Reilly, S. 2010 “Advances in Biporous Wick Desing and Testing for Thermal Ground Planes”, *Frontiers in Heat Pipes*, Vol 1, n° 1, 3001. pp. 1-6.
- Dullien, F.A.L., 1979 “Porous Media Fluid Transport Pore Structure”, San Diego, California,USA, 391 p.
- Faghri, A., 1995, “Heat Pipe Science and Technology” Ed. Taylor & Francis, Washington, USA, 874p.
- Fernandes, C. P., 2002 “Engenharia de Microestruturas: Análise Quantitativa de Imagens e Simulação de Processos Físicos”, Monografia para o Concurso de Professor Adjunto do Departamento de Engenharia Mecânica da UFSC. Universidade Federal de Santa Catarina, Florianópolis.
- Ford, R. A., and Handam, M. H., 1998 “Coupled Parallel Flow Through Composite Porous Layers”, *Applied Mathematics and Computation*. Vol. 97. pp 261-271.
- Innocentini, M.D.M., Salvini, V.R., Pandolfelli, V.C., Coury, J.R., 1999 “ Assessment of Forchheimer’s Equation to Predict the Permeability of Ceramic Foams” *Journal American Ceramic Society*, Vol. 82, n° 7. pp. 1945-1948.
- Kececioclu, I. and Jiang, Y. 1994 “Flow Through Porous Media of Packed Spheres Saturated With Water”, *Journal of Fluids Engineering*, Vol. 116, march .pp. 164-170.
- Marques Filho, O and Vieira Neto, H., 1999. “Processamento Digital de Imagens”. Brasport Livros e Multimídia Ltda., Rio de Janeiro.

8. RESPONSIBILITY NOTES

The authors are the only responsible for the printed material included in this paper.